POLITECNICO DI TORINO

MASTER's Degree in Nanotecnologies for ICTs

MASTER's THESIS

Structural and electronic properties of nano-materials under deformation

Supervisors

Prof. CARLO RICCIARDI

Dr. DAMIEN ALLOYEAU

Dr. RICCARDO GATTI

Dr. HAKIM AMARA

Candidate

MATTEO ERBI'

June 2020

Table of Contents

List of Tables

List of Figures

Acronyms

MD
: Molecular Dynamics

FE
: Finite Element

NP
: Nano Particle

TB
: Tight Binding

Chapter 1

Introduction

The study of electronic and physical properties of nanostructures under deformation: this is the ultimate goal of a project started during this internship but that will continue during three years of PhD. Parallel to the development of the project, there is the formation of a Higher Degree Research student able to manage at several levels the simulation/modelling of different properties at the nanoscale, ranging from the electronics to the mechanics. The internship was carried out in cooperation with the LEM laboratory (Laboratoire d'Etude des Microstructures) that is a joint CNRS-ONERA research unit. One of the research topics at the LEM is the development, the modelling and the characterization of small scale structures. The group I worked with is composed by Riccardo Gatti, an expert in elastic and plastic deformation modelling, and Hakim Amara expert in modelling the properties of nanomaterials.

Physical properties change when size scales, electronic properties in nanoparticles fade passing from those of bulk material to those of a potential well. This is true also for the mechanical properties, which can be very different in nanostructure compared with the macroscale, from the absence of the mechanism leading to strain hardening to the interplay between material strength and features of the nanoparticle, such as size or shape [1].

As stated above the aim is to obtain electronic properties of a nanostructure under deformation. The electronic properties are recovered in this study with a **Tight Binding formalism**, solution that strictly depends on the atom position, it is thus important to know how atoms displace, from the original configuration, after deformation. There are different ways to model nanostructure under deformation, but two are the main factors limiting the choice of the simulation tool to use: the computing time and the validity of the solution. In the context of understanding the better way to carry on the analysis, we decided to implement a **multi-scale analysis**.

With multi-scale approach is meant the analysis with complementary methods at a different scale of the same problem. The mechanical properties in this internship have been analyzed with a **classical model** used for macroscopic analysis based on continuous equation solved with a Finite Element code and a **semi-classical model**, where the problem is modelled with molecular dynamics. The interactions among atoms are determined by the potential and related forces. In the classical representation, forces are linear in space (spring-like interaction), meanwhile as explained in the following chapters in Molecular Dynamics non-linear forces built with non-classical assumptions are taken

into account.

The computing times are very different, ranging from minutes of the Finite Element solution to some days for the Molecular Dynamics simulations, the latter is the most physically correct solution, but the computing time is a strong limitation in the applicability for a large structure.

To verify the accuracy of a finite element solution at the nanoscale, it means to have verified its validity at every dimension. If a result of this kind is achieved, it would set the grounds for an analysis of the electronic properties of objects from the nanoscale to the macroscale, with calculation time within the range of applicability.

The previous works in multi-scale analysis are multiple [2], although they are mainly oriented in the analysis of the plastic region, while here only the analysis of the elastic regime is considered, for sake of simplicity. From our point of view, there are no reasons to expect that a classical model, valid for macroscopic material, holds at the nanoscale: divergence of the results is possible reducing the size of a nanoparticle.

The subject of the analysis are **gold nanoparticles**, chosen for their simplicity, no particular features are expected in the electronic properties and the mechanical properties are a well-known field. It represents a "trial" material, for a future approach applicable to other more interesting materials. Nevertheless, in nanoparticle shape, gold is the best catalyst discovered so far, for application spread from sensing, optoelectronic to biological systems [3].

Molecular Dynamics was new expertise inside the lab, it has been studied together with my supervisors and the developed scripts are attached in the supplementary material. The study of electronic properties was started a few weeks before the report submission, on this subject the work presented is slightly less detailed. The report is divided into three main parts; in the first, a short theoretical review on essential and necessary theory is presented, in the second part you will find the methods that have characterized our study. In the last one, you will find a detailed data analysis, achievements, limits and future perspective.

Chapter 2

Theory

2.1 Molecular Dynamics

Molecular dynamics (MD) is a semi-classical simulation technique that allows to compute many properties in a many-body problem, by means of particle trajectory calculated with classical laws and interatomic potentials constructed in a "quantum" way. One of the interesting characteristics of MD is that simulations are in very similar to real experiments.

The basic idea is that every atom has a potential, which interacts with all other crystal atoms. Therefore each atom feels the potential contribution of the whole structure and this amount can be classically related to force and through Newton's second law, to the position. This process can be repeated iteratively until equilibrium[1] is achieved. Each MD code must follow a few basic steps:

- **Initialization** At the beginning of the simulation the problem must be initialized, i.e. the initial position $\mathbf{r}(t)$ and the velocity $\mathbf{v}(t)$ of atoms must be decided. The initial position will determine the final structure, and the velocity is defined by temperature thanks to the energy equipartition theorem.

- **Force Calculation**. What we want to calculate is the force $\mathbf{f}(\mathbf{r})$ that acts on all the elements of the system, as to observe its evolution. This is done by considering the gradient of the potential $U(\mathbf{r})$:

$$\mathbf{f}(\mathbf{r}) = -\nabla U(\mathbf{r}) \tag{2.1}$$

  whereas potential we should consider the contribution of all the $N-1$ atoms in the structure. A typical example is a pair-wise interatomic potential where we can fully compute the force acting on each atom by simply knowing the distance between them. So, for instance, in a pair-wise inter-atomic potential, knowing the distance between each pair of atoms, we can fully compute the force acting on each atom.

[1] By equilibrium we mean, the condition in which the resultant of the force acting on the single equal atom is zero. This with Newton's second law leads to an acceleration equal to zero.

This is the most time-consuming part of the whole MD simulation, in a system where we consider that each atom interacts only with its first neighbour, the computing time will scale with N^2. In the code I used, the contribution of an atom is considered only if the distances are smaller than a cutoff distance. For systems with a large number of atoms, the speed of the simulation can be increased reducing this radius and therefore considering less contribution, however decreasing the cutoff radius is detrimental to the final result accuracy. More details regarding the potential used in this work will be given in the following.(see section 2.3).

- **Integration**. Once the forces on each atom are calculated, time integration is fundamental to compute the new position $r(t \pm \Delta t)$, it can be done numerically and, we can use, for instance, the **Verlet Algorithm** where considering the Taylor expansion arount t we can write:

$$\mathbf{r}(t \pm \Delta t) = \mathbf{r}(t) \pm \mathbf{v}(t)\Delta t + \mathbf{a}(t)\Delta t^2 * 0.5 \tag{2.2}$$

where a is the acceleration. From this equation, it can be obtained:

$$\mathbf{r}(t + \Delta t) = 2\mathbf{r}(t) - \mathbf{r}(t - \Delta t) + \mathbf{a}(t)\Delta t^2 \tag{2.3}$$

The acceleration can be derived by the force ($\mathbf{F} = m\mathbf{a}$), so the position of any atom at the time $t + \Delta t$ depends only on the force and not on its velocity. This is the most simple, commonly used and effective integration technique, even if many others exist. [4]

Nowadays molecular dynamics is a well-established simulation technique. Therefore, for the analysis of mechanical properties of nanoparticles in this manuscript, we choose to not develop a specific MD code but to use LAMMPS MD code, widely used in the scientific community. LAMMPS stands for Large-scale Atomic/Molecular Massively Parallel Simulator and it has been developed by the Sandia National Laboratories [5]. The use of this program requires to conceive an input script, in which material properties (interatomic potential, masses, crystallographic structure..) and simulation conditions (energy minimization, indentation...) has to be specified. The input code written during the internship is attached in the supplementary material. A.1

2.2 Tight-Binding formalism

Before introducing the potential that we will use to characterize our system thanks to MD, it is necessary to speak about the Tight-Binding (TB) approximation [6]. This formalism will be used not only for the potential construction but also to study the electronic properties when the NPs are deformed. The tight-binding method is a model that allows you to obtain information about the electronic properties of a material. Given its assumptions, it is very useful when applied to s-p-d-materials. Unlike classical methods where the electrons in a metal are considered totally free, in the TB approach, the inverse is done: metallic properties originate from an overlap of atomic wave functions. The lower

this overlap is and the lower is the metallic behaviour and the energy spectrum of the crystal will be very similar to the atomic one, with flat and localized states. It can be shown that the TB Hamiltonian (H) in case of one atomic orbital per atom is:

$$H = \sum_n |n\rangle \, \epsilon_n \, \langle n| + \sum_{n \neq m} |n\rangle \, \beta_{n,m} \, \langle m| \tag{2.4}$$

where $|n\rangle$ is the atomic wave-function in $n-th$ site. As you can see, H is made up of two terms. The first called the atomic level represents the energy level in an isolated atom, ϵ_n equal to $\langle n|H|n\rangle$. The second, called the hopping integrals, represents the wave-function overlap $\beta_{n,m}$ between n and m site. In this way there is compatibility with the atomic description, unlike block or free electron model. $\beta_{n,m}$ can be obtained calculating the following integral $\langle n|H|m\rangle$ or it can be fitted on experimental or ab-initio data as done in the present work.

For the purpose of this work, it is interesting to introduce the concept of the local density of states (LDOS), it is the parameter that we will analyse to understand the electronic properties when the nanoparticle is deformed. A local density of states description is useful in with nanoparticle because we are not interested in certain characteristics of the bulk, but in the behaviour of well-confined regions such as surfaces where many interesting phenomena may occur. The local density of states for a generic atom n is:

$$d_n(E) = \sum_k | \, \langle n|\Psi_k\rangle \, |^2 \, \delta(E - E_k) \tag{2.5}$$

This expression states that every contribution to the density of states $\delta(E-E_k)$ is weighted by the probability $| \, \langle n|\Psi_k\rangle \, |^2$ of finding an electron in a particular base state $|n\rangle$ and the summation spreads over all the k-states with energy E_k and wave function Ψ_k that is a linear combination of atomic states $|n\rangle$. The expression for the total density of states can be reconstructed following $D(E) = \sum_n d_n(E)$.

To calculate the LDOS in a very efficient way, it is useful to introduce an alternative formulation of 2.5, particularly suitable for calculation, based on Green functions G. Assuming that

$$G = \frac{1}{z - H} \tag{2.6}$$

with $z = E + i\epsilon$, H is the Hamiltonian shown in eq. (2.4), E represents the eigenvalues, and ϵ an arbitrary small quantity. The local density of states can be fully recovered as the limit of the Green function imaginary part [7]:

$$d_n(E) = -\frac{1}{\pi} \lim_{\epsilon \to 0+} Im(G_{nn}) \tag{2.7}$$

where $d_n(E)$ is the local density of states of n-th atom. $Im(G_{nn})$ is the imaginary part of a green function. To determine the Green function means to determine the LDOS, there exist different methods to do so but the treatment of such a topic won't be full filled in this report.

2.3 Second moment approximation

The ingredient that characterizes our system, in MD simulations, is the potential. To reproduce the behaviour of a specific material means, to use in the MD simulation a potential with the specific characteristics of the material itself, the electronic configuration is different from atom to atom. In literature there exist many, the most simple one is the well known Lennard Jones, that is totally empirical and not efficient to characterize transition metals but there exists a class of potential perfectly adapted **Embedded Atom Model**, **Finnis-Sinclair** and **Second Moment Approximation** [8]. The approach that we will use is the *Second Moment Approximation* (SMA).

Usually every potential is defined considering two contribution one repulsive ($E_{Repulsive}$) and the other attractive ($E_{Attractive}$) [6]. Thus, the total energy of an atom i is given by

$$E^i_{tot} = E^i_{Attractive} + E^i_{Repulsive} \tag{2.8}$$

The repulsive term is purely phenomenological, and it takes into account for very small distance, core electrons cloud overlap and a strong Coulomb repulsion arise

$$E^i_{Repulsive} = \sum_{i \neq j} A e^{-p(\mathbf{r_{ij}}/r_0 - 1)} \tag{2.9}$$

where r_{ij} is the distance between the first j neigbours, r_0 the equilibrium distance of the considered material. A and p are parameters to be fitted. Usually in literature the attractive term is considered to be the source of binding inside solid. As a result, it is called the band energy. The **band contribution** is the sum of all the occupied electronic eigenvalues. In a TB description, when two atoms interact, two kinds of bonds can be created, bonding and anti-bonding with corresponding energy $E_\pm = \alpha \pm \beta$ where α is the atomic energy and β the overlap integral. If both level eigenvalues are occupied, there is no net advantage in creating a bond. The construction of the SMA is centered around two fundamental hypotheses, the Friedel Model and the Moments theorem.

The **Friedel model** is used to approximate the local density of states[9]. As seen in Fig.2.1, the essence of it, is the possibility to substitute the d-electron DOS with a rectangular shape in energy, instead of the real complex geometry, this is possible thanks to the fact that d-electrons are much more localized compared to the s one.

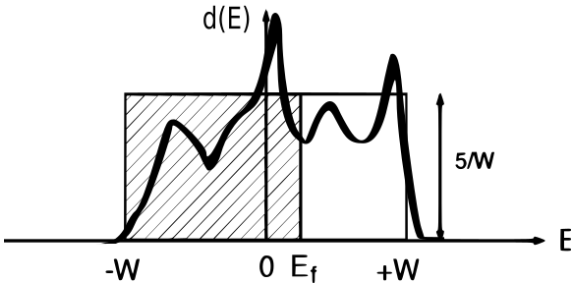

Figure 2.1: Illustrative view of Friedel approximation. $2W$ is the width of the DOS and E_f the Fermi level.

Last is the the **Moments theorem**, introduced by Cyrot Lackmann that without details relates the local density of states moments to specifics of the crystal, but at same time momets are related to hopping integral in a tight binding view. [8] These two concepts together allow to write the energy band, that shows:

$$E^i_{attractive} = -\sqrt{\sum_{i \neq j} \xi^2 e^{-2q(\mathbf{r_{ij}}/r_0 - 1)}} \tag{2.10}$$

this together with the repulsive term (equation 2.9), builds the Second Moment Approximation potential, minimum at a distance r_0, between point r_i and r_j where ξ, q together with A, p are constants to be fitted, that in the analyzed case are specified in the molecular dynamics input code.

2.4 Mechanical properties

In this section basic concepts of linear elasticity and mechanics are reviewed. These concepts are fundamental to introduce finite element analysis in section 2.5 and to compute elastic constants from MD calculations (section 3.1). In linear elasticity, a rigid body is considered as a continuum and homogeneous elastic medium rather than as a periodic array of atoms [10]. To start the discussion, let's introduce the notion of stress and strain.

The **stress** σ_{ij} is defined as the force acting on a unit surface area of a given domain. Being i, j the x,y,z directions, the stress is a 9 component tensor. Indeed a force can be applied parallel to the direction i, and normal to a surface[2], in this case, we talk about normal stress (diagonal components of the stress tensor). Meanwhile, when a force is tangential to the surface, we refer at it as a shear force, generating a consequent shear stress [11]. So, as mentioned above, a force applied on a surface generates stress, and to this stress, a stress field is associated, thus in each point (x, y, z) of the domain, a stress tensor exists.
The definition of **strain** can be directly derived from the **displacement** field. Let's consider a point in position $\mathbf{r}$ that after the effect of a force, moves to the position $\mathbf{r'}$. The displacement is defined as

$$\mathbf{u}(\mathbf{r}) = \mathbf{r'} - \mathbf{r} \tag{2.11}$$

If the displacement is infinitesimal the strain can be defined as the symmetric part of the displacement gradient:

$$\epsilon = \frac{1}{2}\Big(\nabla \mathbf{u} + (\nabla \mathbf{u})^T\Big) \tag{2.12}$$

When stress is applied onto a rigid body, the rigid body undergoes to a deformation. Releasing the loading, if the body returns to its initial configuration, the deformation is called elastic, if permanent deformation has occurred it is called plastic deformation. The stress at which the first event of plastic deformation occurs, in a perfectly crystalline material, is called **critical stress** or **yield stress**. The physical phenomenon underlying

[2] A surface is defined by its normal vector.

plastic deformation in crystalline materials is the formation and/or the movement of **dislocations**. Dislocations are linear defects, and thanks to their movement they allow for the stress field in the crystalline material. In figure 2.2 you can observe an ideal stress and strain experiments, initially the object deforms elastically, and after the yield point deviation from the initial linearity happens.

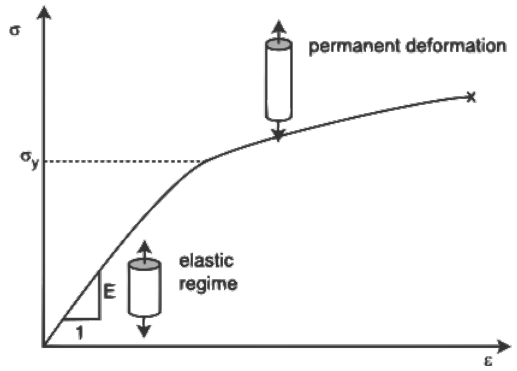

Figure 2.2: Ideal stress and strain plot of an object under tensile loading.[12]

In the elastic regime the generalized Hooke law can be written, stating that for small deformation stress and strain are linearly related [10]. It can be demonstrated that stress and strain are symmetrical), that means that only 6 components of the stress/strain tensor are independent (e. g. $\sigma_{ij} = \sigma_{ji}$). The Hooke law for cubic crystal is:

$$\begin{pmatrix} \sigma_{xx} \\ \sigma_{yy} \\ \sigma_{zz} \\ \sigma_{yz} \\ \sigma_{zx} \\ \sigma_{xy} \end{pmatrix} = \begin{pmatrix} C_{11} & C_{12} & C_{12} & 0 & 0 & 0 \\ C_{12} & C_{11} & C_{12} & 0 & 0 & 0 \\ C_{12} & C_{12} & C_{11} & 0 & 0 & 0 \\ 0 & 0 & 0 & C_{44} & 0 & 0 \\ 0 & 0 & 0 & 0 & C_{44} & 0 \\ 0 & 0 & 0 & 0 & 0 & C_{44} \end{pmatrix} \cdot \begin{pmatrix} \epsilon_{xx} \\ \epsilon_{yy} \\ \epsilon_{zz} \\ \epsilon_{yx} \\ \epsilon_{zx} \\ \epsilon_{xy} \end{pmatrix} \tag{2.13}$$

Playing with maths, from this linear system we can derive the expression of the elastic constant components as a function of stress and strain. This will be useful to calculate elastic constant from MD results (section 3.1).

$$C_{11} = \left[\sigma_{xx} - \sigma_{zz}\frac{\epsilon_{yy} + \epsilon_{zz}}{\epsilon_{xx} + \epsilon_{yy}}\right]\frac{\epsilon_{xx} + \epsilon_{yy}}{\epsilon_{xx}(\epsilon_{xx} + \epsilon_{yy}) - (\epsilon_{yy} + \epsilon_{zz})\epsilon_{zz}} \tag{2.14}$$

$$C_{12} = \frac{\sigma_{zz}}{\epsilon_{xx} + \epsilon_{yy}} - C_{11}\frac{\epsilon_{zz}}{\epsilon_{xx} + \epsilon_{yy}} \tag{2.15}$$

Assuming we are dealing wiht an isotropic material:

$$C_{11} = C_{12} + 2C_{44} \tag{2.16}$$

Using this relation together with the most general form of a fourth order isotropic tensor:

$$C_{ijkl} = \lambda\delta_{ij}\delta_{kl} + \mu(\delta_{ik}\delta_{jl} + \delta_{il}\delta_{jk}) \tag{2.17}$$

we can identify the Lamé parameter λ and μ as

$$C_{11} = \lambda + 2\mu \tag{2.18a}$$
$$C_{12} = \lambda \tag{2.18b}$$
$$C_{44} = \mu \tag{2.18c}$$

and it follows that

$$\sigma = \lambda tr(\epsilon) I + 2\mu\epsilon \tag{2.19}$$

where $tr(\epsilon)$ is the trace of the strain tensor ϵ, and I is the identity matrix. Evaluating separately C_{44}, C_{11}, C_{12} it is possible evaluate the anisotropy it is usually defined the **anisotropic factor** A:

$$A = \frac{2C_{44}}{C_{11} - C_{12}} \tag{2.20}$$

Another useful parameter is the **Bulk Modulus** that is a measure of how a solid is resistant to an isotropic compression. In an isotropic material, it can be shown that [10]

$$B = \frac{1}{3}(C_{11} + 2C_{12}) \tag{2.21}$$

2.5 Finite Element

The Finite Element Method (FEM) is a numerical technique commonly used to solve physical, mathematical and engineering problems that can be described by partial differential equations (PDE). The domain Ω in which PDEs are defined is discretized into a mesh. In our case, dealing with with a 3D structure, the domain is divided into tetrahedra or hexahedra elements. The solution of the problem is calculate on the mesh nodes. Typically for simplest mesh elements, nodes are the corner of the chosen elements. Boundary conditions has to be properly imposed to define a boundary value problem, to be able compute a unique solution of the given problem. The environment chosen to solve PDE is FEniCS[13][14], a popular open-source computing framework. FEniCS enables users to quickly translate physical and engineering models into an efficient finite element formulation, thanks to a high-level Python and C++ interface.
Let's start identifying PDEs that govern the under analysis system. As we did before for MD we want to probe mechanical properties and thus reproduce an indentation experiment. The equation of motion for a body under external loading, considering only the x direction, shows as [10]

$$\rho \frac{\partial u^2}{\partial^2 t} = \frac{\partial \sigma_{xx}}{\partial x} + \frac{\partial \sigma_{xy}}{\partial y} + \frac{\partial \sigma_{xz}}{\partial z} + f_x \tag{2.22}$$

where f_x represents the body force, due to cohesive phenomena, the second contribution is due to contact forces, that exist only at the surface. In static condition and considering the contribution in all directions the previous relation can be seen as[15] [12]:

$$-\nabla\sigma = \mathbf{f} \tag{2.23}$$

that together with a generalized form of the Hook law eq: 2.19 and the definition of strain of eq:2.12 give rise to a second order partial differential equation where the displacement

u is the unknown function on the domain Ω. For the sake of simplicity we will keep the equation separated even in the code.
In the next lines the mathematical basis of a finite element model[16] is briefly recalled since it is fundamental for understanding how a FE code works and how to interpret the results. It is common in an FE approach to reduce the differential equation order, a *weakformulation* of the initial problem can be written. In our case this is possible applying the divergence theorem:

$$-\int_{\Omega}(\nabla\cdot\sigma)\cdot v=\int_{\Omega}\mathbf{f}\cdot v \tag{2.24}$$

where v, is called test function, it is not the unknown of the system, but something that exists only virtually to write down the problem, it will be set to zero in regions where boundary conditions are imposed, this allows to further simplify the formulation. Thanks to the previously mentioned theorem one obtains[3]:

$$\int_{\Omega}\sigma:\epsilon(\mathbf{v})=\int_{\Omega}\mathbf{f}\cdot v+\int_{\partial\Omega_T}\mathbf{T}\cdot v \tag{2.25}$$

Where the quantity $\mathbf{T}$ is known as the traction or stress vector at the boundary defined as $\sigma\cdot\mathbf{n}$, $\mathbf{n}$ normal vector to the surface.

There are mainly three different steps that outline the characteristics of the method:

- **Mesh creation** Mesh must be created dividing Ω in elements (3D tetrahedra in our case). in each mesh element the unknown u is approximated with a linear function of the type,

  $$p(x_1,x_2,x_3)=a_0+a_1x_1+a_2x_2+a_3x_3 \tag{2.26}$$

  which is a linear function for a three dimensional domain. A linear function in 3D domain is uniquely determined by its values on four different non aligned points $p_j=(a_0,a_1,a_2,a_3)$, these three values are called local degrees of freedom, the ensemble of all the linear functions over our domain is a vector space. In FE we approximate the solution with a linear one over the elements, it is usually written as

  $$u_h=\sum_{j=1}^{N}u_h(p_j)\phi_j(p_i) \tag{2.27}$$

  where $u_h(p_j)$ is the function calculated at the nodal value p_j uniquely determined by a set of three coefficients. The function $\phi_j(p_i)$ is Kronecker delta equal to 1 if $i=j$ and it is a basis for the space called V_h.

- **Boundary conditions** A PDE can be correctly solved only together with a boundary condition, in our case we imposed BC directly on displacement, zero displacement on the NP bottom and the desired value at the top. These are called **Dirichlet condition** being directly imposed on the unknown function.

[3]The notation used follows the UFL standard, the symbol [:] stands for inner product, the symbol [·] for dot product. More information can be found in [17]

- **The discrete variational problem** The ultimate goal of a finite element model is to calculate the value of our unknown in the mesh nodes. Therefore, we have to create a problem related to the variational continuous previously exposed. The solution will be obtained in the V_h space and the problem is reduced in computing the unknown function, u_h, at the nodes.

Chapter 3

Results

The theoretical and methodological background introduced in chapter 2 is now applied to study gold nanoparticles,to determine their physical and electronic properties under deformation. The goal is to analyze gold nanoparticles under loading (indentation) with different simulation methods (MD and FE) and finally to compute the electronic properties, as already explained in the introduction 1.
Before analyzing the behaviour of a nanoparticle, it is useful to check bulk gold properties to validate the potential used in MD simulations. This step is useful for determining the crystallographic structure of gold and, most importantly, its mechanical properties such as elastic constants, bulk modulus, essential input parameters for finite element analysis. From section 3.3 onwards the indentation experiments, and to the analysis of the mechanical properties gold nanoparticles of several dimensions, with both FEnics and LAMMPS codes is presented.
The final part concerns the electronics properties analysis of gold NP during deformation.

3.1 Crystallographic structure

As previously mentioned, a standard molecular dynamics code calculates the position of atoms at the time $t + dt$ considering the forces acting on atoms at t. This iterative process continues until an equilibrium position is reached. Every MD simulation presented in this manuscript has been conducted at a temperature close to zero, in fact it is not a problem to perform simulations at a finite temperature, but fluctuations in the output due to thermal motion would be present. The contribution to the total energy of an atom, considering the kinetic energy negligible, is only described by the potential. The **equilibrium position** will be the position where the forces acting on the atom are equal to zero, this happen in the minimum of the potential. From solid state physics we know that there are different crystallographic configurations in which atoms can organize themselves (simple cubic sc, face centered cubic fcc, body centered cubic bcc ...).

In first analysis we verified the validity of the SMA potential developed for Au with LAMMPS, finding the crystallographic configuration with minimum energy, which corresponds to the most stable structure and therefore the one observed in the real material. In addition, the **lattice parameter** was obtained and compared with the experimental one.

To look for the equilibrium position we must introduce the concept of **cohesive energy**. The latter is defined as the energy to be provided to an atom, such that you separate it from the lattice, or more trivially how the potential in the equilibrium position is deep. The crystalline configuration with the lower cohesive energy is the most stable one.[10]

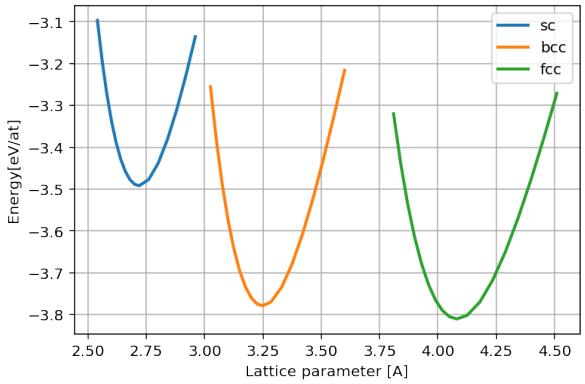

Figure 3.1: Cohesive Energy (eV/at) as a function of the lattice parameter for different Au structures : simple cubic (SC), body-centered cubic (BCC) and face-centered cubic (FCC). Results obtained with our SMA potential.

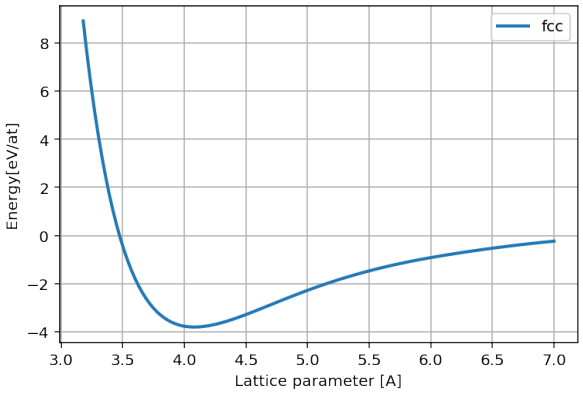

Figure 3.2: Cohesive energy of the FCC structure which is the most stable configuration. According to our SMA potential, the cohesive energy is equal to -3.81 eV/at

In figure 3.1 the cohesive energy of three different crystalline configuration is shown. Coherently with literature [10] Gold is more stable in the fcc configuration. In figure 3.2 the potential energy in fcc configuration is shown as function of distance between atoms. This result is obtained wiht the SMA potential of 2.3 and looking at equation 2.1 the repulsive and attractive contribution are clearly visible.

3.2 Elastic Constants calculation

Once the optimal configuration of the bulk material has been found, it is possible to proceed with the computation of fundamental parameters for FE simulations, such as elastic constants.

For this simulation a compressive strain ϵ_{zz} in z direction is applied on a simulation box with 500 atoms in fcc configuration and the boundary condition to simulate a bulk system, has been imposed. Extracting the values of stress $(\sigma_{xx}, \sigma_{yy}, \sigma_{zz})$ and strain$(\epsilon_{xx}, \epsilon_{yy})$, two out of three elastic constants (C_{11} and C_{12}) can be calculated using eq. (2.14) and (2.15). For the computation of C_{44} a shear strain has been applied to the simulation box. Properly measuring the resulting shear stress C_{44} can be straightforwardly calculated. The Bulk modulus has been obtained with eq. (2.21) and the lattice constant as explained in the previous section 3.1.

As evidenced by Table 3.2, the data obtained with SMA potential shows a good agreement with the experimental data. The only substantial difference is represented by

	B[GPa]	C_{11} [GPa]	C_{12} [GPa]	C_{44}[GPa]	a[Å]	$E_{coh}[eV/atom]$
SMA	171	180	167	44	4.08	-3.81
Experiments	171	201.6	169.7	45.4	4.08	-3.81

Table 3.1: Physical properties of Au with the FCC structure. Comparison of our SMA potential with experiments[10].

the value of C_{11}. However the difference with C_{11} is about 10%, so we can claim that the SMA potential reproduces correctly the elastic properties of Au FCC and it is perfectly suited for the present study.

3.3 Indentation

The indentation experiment is the process by which a loading is applied to a surface of a given material by an indenter (and object mach harder then the tested material). Typically, to perform indentation in nanoparticles, a tip (usually made of diamond and with radious $\sim$ 100 nm) is pressed against a nanoparticle surface with the final goal to probe its mechanical properties. This experimental technique can be reproduced by simulations. Indentation simulations are useful to investigate the physical elementary mechanisms underlying to the observed mechanical properties. Nowadays several research groups work on this field, from both sides. Experimental indentation on a nanoparticle can be performed with two main different techniques: Scanning Probe Microscopy[18] (the nanometric tip can be used both for indentation and for imaging) and/or the in-situ Transmission Electron Microscopy nano-indentation. In particular the last one provides the tools for a real time characterization of the nano or micro-structure and defect behavior with an high spatial resolution and the possibility of correlating load–displacement curves with changes in the nano-structure. [19]
These experiments are usually supported with numerical simulations both to confirm results confirmation and to better understand the underlying physical mechanisms. The main tool to model nano-indentation is Molecular Dynamics[20][1][18][2], the principal limit of this technique is the computing time, simulation of large nano-structures can last $\sim 10^5 s$ and more. An intriguing alternative are classical methods, based on solving partial differential equation where a simulation run is less demanding, $\sim 10^3 s$.

The present study focuses more on the analysis of the tools with which we can simulate an indentation experiment (MD and FE), rather than the fine analysis of physical properties analysis. Furthermore a physical phenomena such as the size effect has been investigated even if not strictly related to the objective of the internship. During the process of indentation of an object, the deformation is initially reversible in the elastic region, where the Hooke law holds, then the deformation becomes plastic, irreversible with the introduction of defects (dislocations) inside the material.

One can argue that figure 3.3 does not look like figure 2.2, this is because the two experiments are made on object with different size, the experimental one on a macroscopic sample, while MD simulations were performed on a nanoparticle. In nanometric object a single plastic event can drastically impact stress vs strain curve [2]. In MD an FE simulations **displacement-control mode** is applied. this means that every simulation

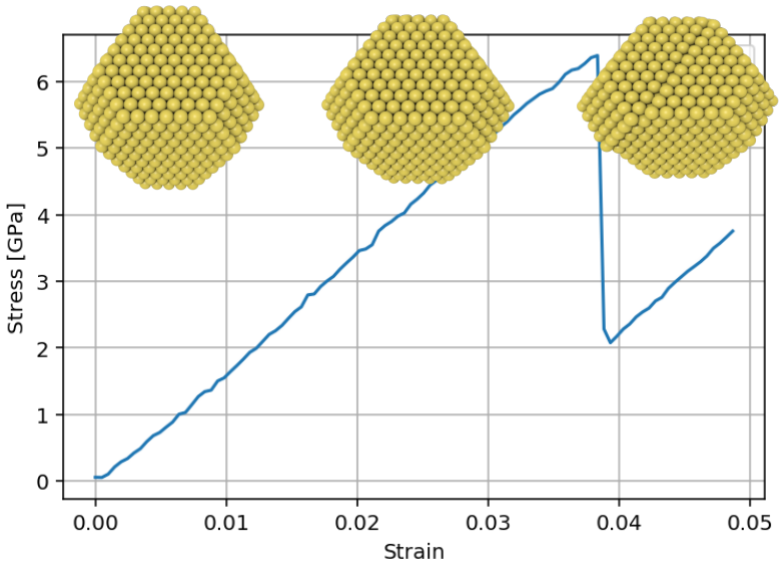

Figure 3.3: Example of a displacement control stress-strain trend, with nanoparticle underlying the compression

step the indenter is displaced by a fixed value,a new boundary condition is applied, imposing a fixed displacement on the NP. As a result, in the MD simulation, where prediction on the plastic regime can be made, the load drops precipitously in the simulations after each dislocation event, because dislocation nucleation changes drastically the shape of the nanoparticle.

This study focuses on the linear region (equation 2.25 cannot make prediction about the plastic region) of the stress vs strain curve. In particular an evaluation of a full stress map in every simulation step and of the true stress-strain curve is made, with both continuous and semi-classical models.

3.3.1 The nanoparticles

As previously mentioned, the aim is to investigate mechanical and electronic properties with different simulation techniques. Gold nanoparticles of size in the $[2-20]$ nm range are studied. The shape and size of the NP is very important, because structural and electronic properties depends on it. For Gold, the most stable configuration, in the discussed size range, is the *truncated dodecahedron* [21],but due the wider number of literature available we choose the **Wulff structure**. The shape of the analyzed nanoparticle in function of the number of atoms is defined using a code able to reproduce the Wulff construction. The equilibrium structure corresponds with the polyhedron that encloses all the atoms, ensuring that the total surface energy is minimum. [22] The final shape can be observed in figure 3.4 where different facets are present : (001) and (111). The color code stands for the coordination number, post-processed with OVITO [23](a very popular tool to post-process MD data). Larger the coordination number is, lower the total energy of the atom will be because the coordination is related to the number of neighbour and thus to

the existing bonds. Atoms create bonds only if it is energetically convenient for them. In figure 3.5 are presented the NPs of different sizes used in this work.

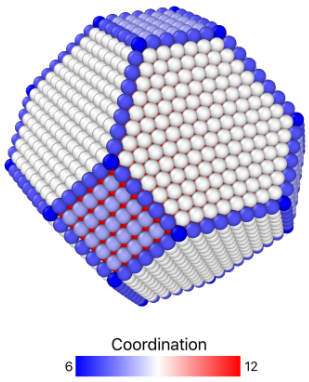

Figure 3.4: Coordination number in Wulff structure where different sites on surface can be identified : vertex, edge, (001) and (111) facets.

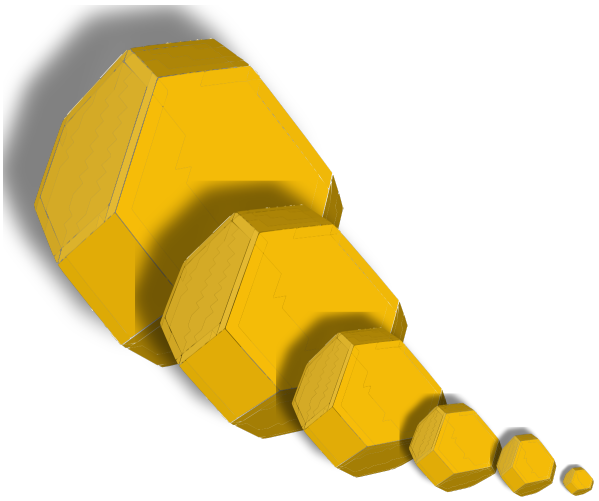

Figure 3.5: Different size of the nanoparticle ranging from 2 to 20 nm. From the smallest to the biggest we used 2, 4, 6, 10, 15, 20 nm.

3.3.2 MD indentation

Indentation was modeled in similar way to [20][1][18][2][24] by considering a NP in the center of the simulation box, with periodic boundary condition. Therefore the NP must be at least 10 Å far from the box side to not be affected by the periodic boundary conditions. the Indenter and substrate are simulated with two rigid infinite planes, for simplicity and parallel to the (001) plane as seen in Figure 3.6. The effect of an indenter is implemented by introducing in the MD simulation fictitious forces, in our case we used a quadratic repulsive force

$$F(r) = \begin{cases} -K(r-R)^2 & \text{if } r < R \\ 0 & \text{otherwise} \end{cases}$$

where K is a constant set to $K = 1000$ eV.Å^{-3}, in agreement with previous works in literature, and $r - R$ is the distance between the indenter plane and the NP atoms. The moving indenter applies a strain rate in a range $[10^8 - 10^9]s^{-1}$ that corresponds to an indenter moving speed of $[2 - 20]m/s$, it is important that this velocity is lower than the speed of sound in Au [1, pag. 5206], this allows atoms to reorganize themself before a new displacement is imposed. During experiments the indenter moves with a speed of about $\sim [0.1 - 0.01]\mu m s^{-1}$ [19, pag. 1136], using such values MD simulations are uviablen they will take too long. The previous approximation (strain rate of about $[10^8 - 10^9]s^{-1}$) allows us to avoid this problem. The cutoff radius chosen is $\sim$ 7Å, this choice can be

justified with figure 3.2, where it is shown that the contribution of potentials become almost negligible at distances > 7Å.

In the process of energy minimization, with a standard MD code, atoms adjust their position exchanging kinetic and potential energy. if there is no loss of energy from the simulation box, we are dealing with with NVE ensemble. In many other application it can be more useful to work with different condition, so in different ensemble. The first constrain that has to be added is the a thermostat, needed both in the NVT and in the NPT ensemble. This is fundamental if we want to avoid oscillation in the particle temperature. From a statistical mechanical point of view, we can impose a temperature on a system by bringing it into thermal contact with a large heat bath.
There are two main approaches to implement a thermostat in a MD code. the first one, Andersen approach, allows to reach constant temperature by stochastic collisions with a heat bath. the second one **Nose-Hoover**, provides a new reformulation of the classical equation of motion based on the introduction of artificial coordinates and velocities. In our simulation we proceed by using the canonical ensemble (NVT) with a Nose-Hover thermostat. [4, pag.139-158]. The input code written use for modeling indentation experiment with MD can be found in the supplementary material A.1. The methods to post-processing the two most important quantity needed for our analysis are explained in the following.

- **Stress Map** LAMMPS provides the tool for the **per atom stress** computation, this allows the construction of a complete stress map, during the simulation. The main contribution is calculated by means of the Virial theorem, which takes into account all the inter-atomic interaction, in which the pairwise contribution is the main term. The computed stress per atom is a per unit of volume quantity, it needs to be divided by the per atom volume. This in LAMMPS can be done with the Voronoi tessellation, this process is still under analysis.

- **True Stress and strain** Given the non-homogeneous distribution of stress, it is necessary to identify a macroscopic quantity that allows to analyze the overall behavior of the structure, the **true stress compression**. To obtain this quantity we must use an average value, calculated knowing the force appliedF_{001} by the indenter and surface contact area A_{001}.

$$\sigma_{true} = \frac{F_{[001]}}{A_{(001)}} \tag{3.1}$$

  The contact area quantity is a not well defined concept, and many ways exist for its calculation, but all of them follow the same recipe[25, pag.7-9]. Firstly, one must *Identify the Atoms in Contact with the indenter*,(see figure 3.6). In our case we have chosen all the atoms at a distance of maximum 1 Å from the indenter, not finding a remarkable differences in the elastic region by slightly varying this parameter. Secondly, knowing contact atoms, one must *compute the contact area*. To evaluate this area we have chosen to compute a Delaunay triangulation of the points define by the coordinates of atom centers at each indenter displacement.

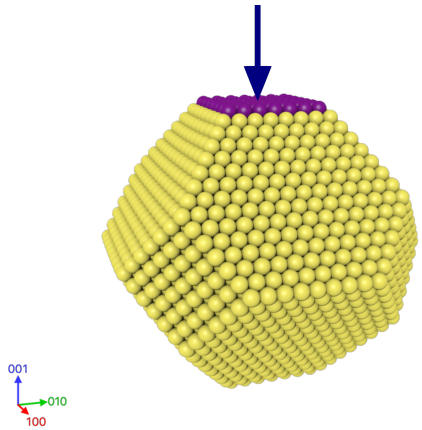

Figure 3.6: Atoms in contact with the indenter.

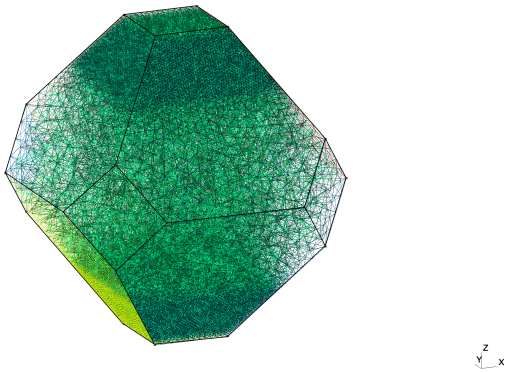

Figure 3.7: Mesh built for the Finite Element simulation.

3.3.3 FE indentation

The indentation process using a finite element model has been simulated on FENICS and following the guidelines outlined above [2.5]. Here below I report practical details on the development of FE indentation model. The code is inspired by the examples found in [15],see A.2 for the complete documentation.
The creation of a **mesh** has proved to be a fundamental step for obtaining results comparable with MD. The mesh must be three-dimensional and have the shape of a nanoparticle. The more refined the mesh is the more precise the solution will be but, at the same time, the computing time to solve the FE problem will increase. A non uniform mesh can thus be implemented with more points on the regions near the contact surfaces, where we expect the highest concentration of stress (see Figure 3.7).

The problem is posed as in equation (2.25), imposing fixed displacement on the z direction of the top (001) boundary to mimic a plane indenter. The displacement values in the FE model were chosen by observing the limits of linearity (yield point) of MD simulations for each nanoparticle. Following the discussion in section 2.4 we considered the material as isotropic, thus $c_{44} = \mu$ and $c_{12} = \lambda$, so from table 3.2 $\mu = 44$ GPa and $\lambda = 167$ GPa. It can be argued that gold is an anisotropic material with anisotropic factor $A = 3$[1]. Even if Au is anisotropic, one can deal with an effective isotropic media calculating effective μ_R and λ_R (Reuss average of elastic constants) media[26]. In this study the approximation of isotropic behavior is chosen, for simplicity, but the analysis will be further improved in the future.

Similarly to what has been done previously, we post-processed, on all NPs,two types of data, which are the **stress map** and an **effective elastic constant**. The stress map is obtained by solving the linear system at each point of the mesh, and then interpolating the points of the mesh with a linear function.

For effective elastic constant is meant the ratio between true stress and true strain in

[1]This value can be calculated from the definition in section 2.4 using the data provided in table 3.2

the z direction. The true strain was easy accessible, because we control the displacement as a boundary condition. For the true stress calculation, the path followed is similar to the one used in the MD indentation. The only difference lays in the force calculation, that this time is not straigthforward, we had to compute the reaction force generated by the plane indenter on the top surface (where the loading is applied).

3.4 Stress-strain curve in Nanoparticles

Firstly the true stress-strain trend obtained with MD is presented. The methods used in this section are the one explained in section 3.3.

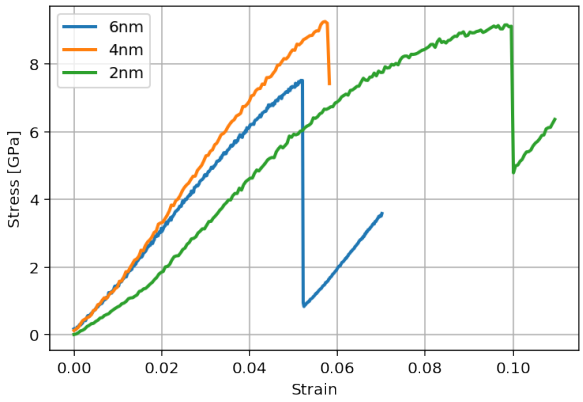

Figure 3.8: Stress strain curve from MD simulations, small nanoparticles.

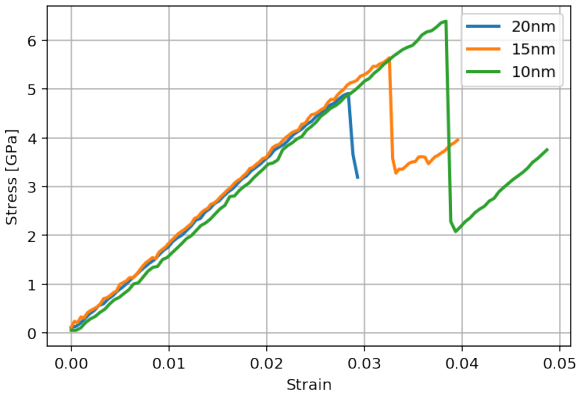

Figure 3.9: Stress strain curve from MD simulations, large nanoparticles.

In figure 3.8 and 3.9 the true stress-strain up to the first **dislocation** event is shown, the drop that can be observed in the stress, is due, as previously explained, to the onset of plastic deformation. In the smallest nanoparticles (left hand side) deviation from linearity is observed even before the dislocation events (evident in 2 and 4 nm size), this can be traced back to the influence of the surfaces on the mechanical behavior inside the nanoparticle, meanwhile the largest NP keep a linear trend up to plastic deformation.Very interestingly, we can observe that our calculations reproduce very well trends similar to those found in the literature, as seen in figure 3.10 [20].

In figure 3.11 the critical yield stress extracted from figure 3.8 and 3.9 is plotted to show the **size effect**. As a critical stress we consider the maximum stress reached, before the first dislocation event. Increasing the nanoparticles size implies a reduction in the critical stress. This trend can be fitted with an exponential function of the type $\sigma_c = A \cdot d^{-B}$ where A and B are fitted values equal to 11.8 0.26 respectively, while d is the NP size. A Comparison with the literature shows that different results has been obtained in [1] ($B = 0.74$), where gold nanoparticle are indented on the (111) surface: the size studied are similar but NPs have a different shape (Winterbottom shape).
On the other hand, in [20] it has been shown that critical stress is highly shape-dependent (see figure 3.10). In [20] silicon nanoparticles, of different shapes, have been indented

on different facets, finding $B = 0.13$ for NPs indented on (111) surface. To confirm this dissertation in [24] it has been shown that the size effect in [111] direction is **not dependent on the material**. Yosi Feruz and Dan Mordehai have shown that Wulff nanoparticle of different material (Al, Au, Ni, Ag and Cu) present the same size size effect with an exponent $B \sim 0.5$, when indented on (111) surface. See figure 3.11, where the comparison with our results is plotted. The critical stress value dependence on multiple factors (size, material, shape, indentation plane and choice of potential) makes difficult to have clear conclusion. Moreover we have to consider that most of the literature analyse the (111) surface, it is not possible for us to make comparison. Possible deviations of the exponential behaviour can be due to the small number of samples considered, to different potential used. More importantly, our study shows that a size effect is clearly observed, with comparable order of magnitude with respect to the data reported in the literature. As previously mentioned a strong effective factor in studying the size effect is not only the material itself but also the choice of the potential for MD calculation. We have verified, not reported here, that different potentials (SMA and EAM) were providing the same size effect but with slight different value the critical stress for a given NP size.

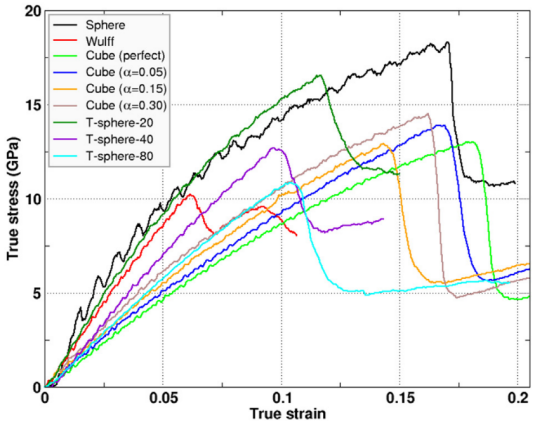

Figure 3.10: Molecular Dynamics simulations extracted from [20], the nanoparticle size is in the range $10 - 50$ nm

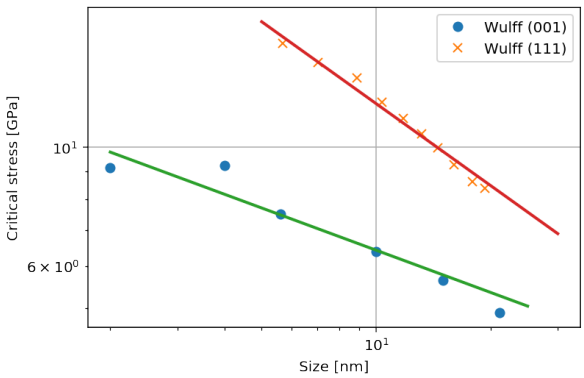

Figure 3.11: Comparison between Molecular dynamics simulation extracted from [1] and the results obtained with the previously explained methods

Now we focus on FE calculations. Given that with equation (2.25) only the linear behavior can be recovered a second plot (figure 3.13) is proposed where the comparison between the effective elastic constants obtained with the two different tools is shown. For the MD simulation this values has been obtained linearly interpolating the stress-strain from 0 to the critical stress, even if some nanoparticles (2 and 4 nm) presents non completely linear trend. This to have a coherent description for all the NP sizes. In figure 3.12 you can see the FE solution compared to the MD one.

The two descriptions are in good agreement, with relative errors $< 10\%$. The exception are the 4 and 15 nm nanoparticles, where the results seam to diverge. In the 4 nm case a deviation from the general trend is detected both in MD an in FE calculations. For the FE case, this deviation can be due to a poorly created mesh, post-processing errors in determining the contact area between the indenter and the NP, or to particular phenomena

that linear isotropic elasticity does not take into account.It is clear that in the near future it will be useful to study precisely why such a phenomenon is observed. However, given that there is no atomistic description via FE, we can think that the area ratio is at the origin of this very particular trend.Consequently, these results are quite impressive because it shown that classical laws (linear elasticity) can hold up to the nanometer scale without strong deviations.

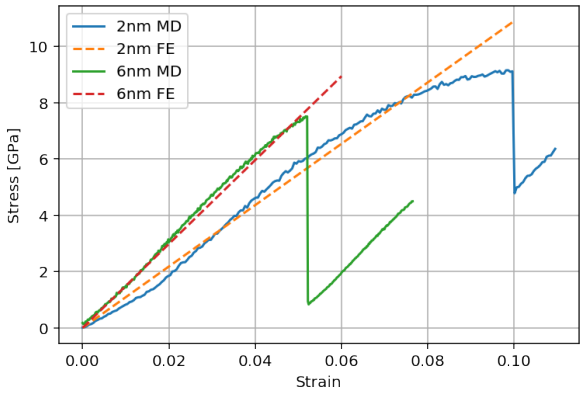

Figure 3.12: Comparison between FE and MD stress-strain trend for 2 nm and 6 nm NPs

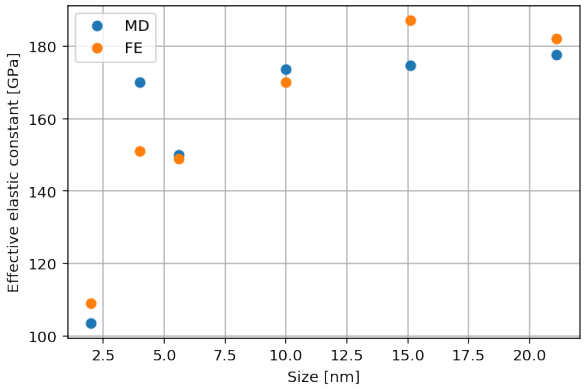

Figure 3.13: Effective elastic constant, comparison between FE and MD results.

In the following we analysed the stress map, the methods applied are the one exposed in section 3.3. The stress maps features (shown in figure 3.14) are very similar, both for the stress distribution inside the nanoparticle and for the order of magnitude. The nanoparticle analysed is the 15 nm size, but similar results has been observed in all the NPs. The stress map shown in figure 3.14, were carried out under the same strain value and considering a strain corresponding to the critical stress, therefore the point of maximum stress inside the nanoparticle.

The central area is characterised by negative stress, which corresponds to a compression of the atoms and it can be viewed considering that the strain along z direction is negative (atoms are moving downwards, see the generalised Hooke law 2.19). Concerning the features, stress is concentrated more in a conical region, starting from the corners where the maximum value is observed. The stress value obtained with MD is not correct at the surfaces, as stated in the methods, LAMMPS output for stress per atom command is a per unit of volume stress. Atoms at the surfaces do not have the same volume as the bulk one, the technique to calculate the per volume per atom called Voronoi tessellation does not work perfectly for surface atoms. The results obtained are still not satisfying at the surface and an improvement is needed.

As mentioned before, this study is mainly focused on elastic properties. As a conclusion, we present the plastic regime observed only through atomistic simulations. In figure 3.15 you can see the stress map of the dislocated 15 nm nanoparticle obtained with LAMMPS visualized with OVITO, two dislocations can be viewed one at the top and the other at the bottom. The nucleation of dislocations causes a very high concentration of stress in one point, compared with figure 3.14 but you can see a total reduction of compressive stress

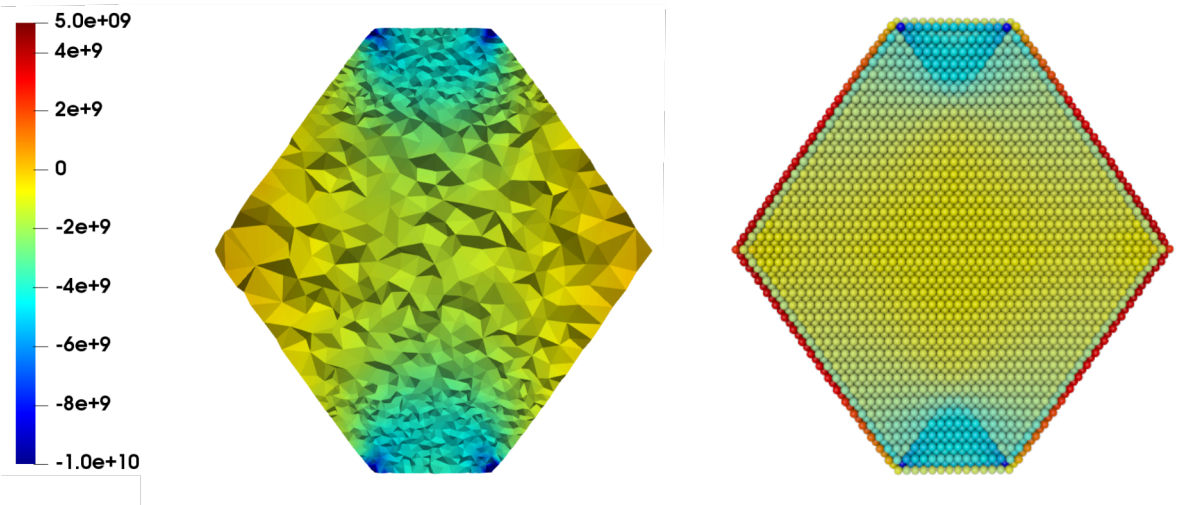

Figure 3.14: slice along the direction [100], 15 nm size nanoparticle for FE an MD respectively. The quantity displayed is σ_{zz} in (Pa), stress tensor component.

on the entire nanoparticle, thanks to the formation of a dislocation atoms can recover a position much closer to that of equilibrium, and then relax the structure. It is interesting to note when a dislocation in a crystalline material (figure 3.16) atoms are rearranged. In figure 3.16 atoms at the bottom are stretched (positive strain and positive stress) and atoms at the top compressed (negative strain and negative stress). This match the features present in figure 3.15, where stress has been relived in the NP by the presence of the two dislocations, in comparison with figure 3.14 .

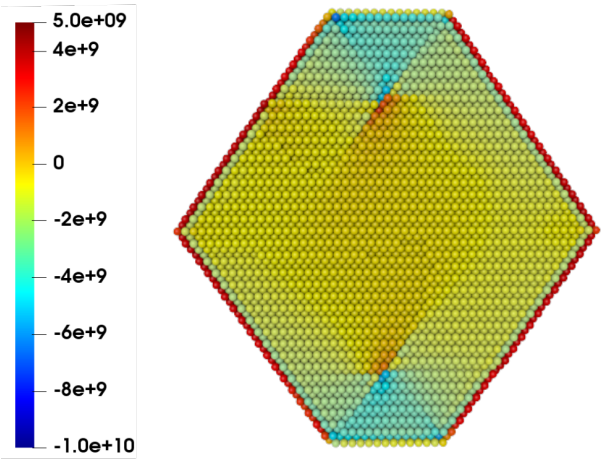

Figure 3.15: dislocation, 15 nm size nanoparticle ,the quantity displayed is σ_{zz} in (Pa), stress tensor component.

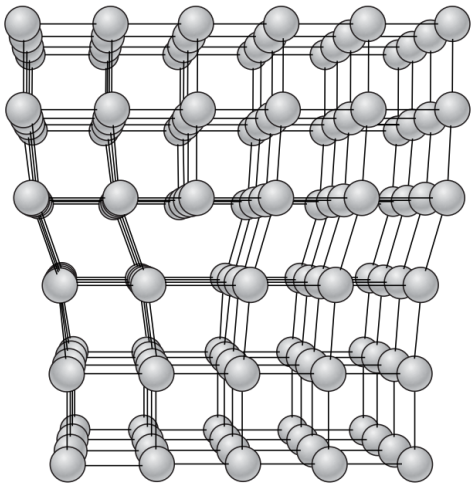

Figure 3.16: atom rearrangement due to an edge dislocation [10]

3.5 Electronic properties

In the following section the electronic properties of nanoparticles, under deformation, are analyzed. The local density of states, in different points of the nanoparticle at different loads, has been extracted. The methods followed for the development are those proposed in section 2.2, which have been applied with the help of Hakim Amara for a lack of time. The tight-binding formalism has been applied to the five d-orbitals, considering that the electronic gold configuration ([Xe] 4f14 5d10 6s1) is totally occupied, using as atom positions input the output from LAMMPS. No particular features are expected except a dependence of LDOS itself on NP deformation. The choice of gold has been done because it is one of the simplest and most documented materials in atomistic simulations, as stated already it is a trial material. Here below the local density of states on the (111) and (100) facets (figure 3.18 and 3.17 respectively) are analyzed but in the supplementary material also edge bulk and vertex are shown. The analysed nanoparticle is the 6 nm size, and three different configurations are shown: zero loading, critical loading and half critical loading.
A recurrent feature is the presence of a gap (around $\sim 1ev$, this could be consistent with a quantization of levels within a nanoparticle, which behaves as a potential well.

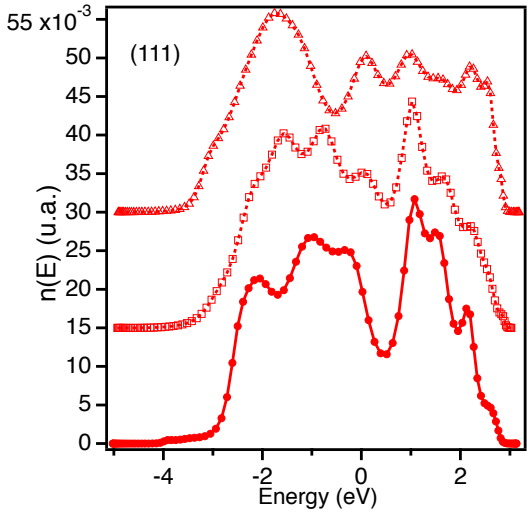

Figure 3.17: (111) local density of states, starting from the bottom [0, $\sigma_c/2$, σ_c] external stress.

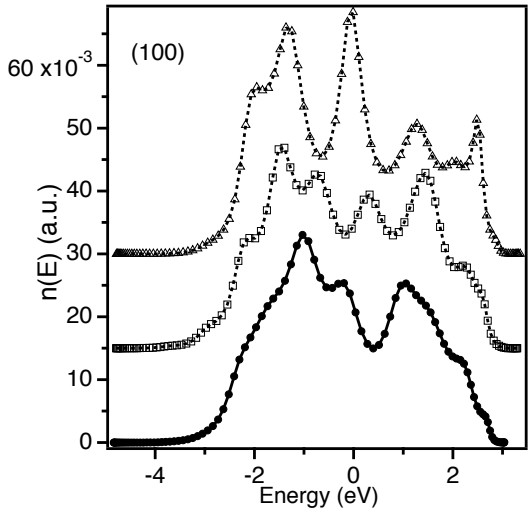

Figure 3.18: (100) local density of states, starting from the bottom [0, $\sigma_c/2$, σ_c] external stress.

Looking at all the extracted figures it is interesting to observe why the Friedel approximation holds and also why the second moment approximation can be considered as a good approximation of the atomic potential, the LDOS is really well confined in space a rectangular shape approximate quite well our results.The most interesting point is that simple very small elastic deformations, drastically change the electronic properties. Such effect, perfectly highlighted thanks to our electronic structure calculations, is very encouraging since it shows how sensitive the local electronic properties of nano-objects are to local deformations. The next step, not presented here, is the reconstruction of the

local density of states starting from the displacement field, solution of the finite element calculation, observe and compare the differences with previous illustrated results.

3.6 Conclusion

In this report, many goals have been achieved. Starting from the analysis of the data obtained with LAMMPS, we obtained lattice parameter, cohesive energy, bulk modulus and elastic constants consistent with the literature, which confirm that the potential used is suitable for the study of nanoparticle under deformation. An exception is the C_{11} elastic constant value, but refining the way in which it is calculated this value can be refined . Secondly, in the analysis of nanoparticles we observed a size effect, finding a good agreement with the literature, although, indentation on different surface and a larger number of samples could help to have a wider understanding of this phenomenon.

Concerning the **multi-scale approach**, we have verified its effectiveness. The computation time for nanoparticles larger than 20 nm, with Molecular dynamics, has proven to be time consuming (3-5 days). While a finite element solution can be provided in a few minutes.

Regarding the analysis of finite element solutions, we can also confirm the consistency with the results obtained with Molecular Dynamics(Figure 3.13), not only the order of magnitude but also the general trend can be recovered, caution is still needed in the conclusions, as there are many aspects that need to be improved. More than everything else, our study shows that it is possible to directly study the elastic properties of NPS via FEs. The approach at the atomic scale (which is longer) will, above all, make possible to clarify and better understand the physical mechanisms at the origin of the results

As mentioned above, also the results obtained on the local density of states are very satisfactory, deformations of less than 6 % can induce significant changes in the final result. As already stated the results shown refer to the displacement field extracted from Molecular Dynamics, but the convergence of the stress map in figure 3.14, make us positive to possibility of fully recover correct electronic properties from a classical-macroscopic solution of the deformation problem, with computation time at the application scale, ranging from the nano to the micro scale.

Other considerations and possible improvements follow. In stress map analysis, it is necessary to consider the volume of atoms with Voronoi tasselation and make the stress map more homogeneous (mainly at the surface). Concerning the study of the effective elastic constant, it is necessary to understand the optimal isotropic equivalent system (or to move to an anisotropic description) to our anisotropic one, more accurate values of μ and λ are needed. From a purely technical point of view, the indenter is now simulated as a plane. It should be modelled as similar as possible to a real one, in order to make the theoretical data more comparable with the experimental ones. Moreover for a wider understating of the physical phenomena underlying deformation, indentation on different crystalline plane and on particle with different shapes needs to be performed.

The future perspectives of this approach are wide. This approach will be extended in the non linear region (plastic behaviour), and electronic properties will be analysed more in detail to understand strengths and weaknesses of this method. As seen in this work, simple elastic deformations strongly modify the electronic properties. The ultimate goal

will be to understand these modifications and to succeed in modulating in engineering the electronic properties of materials under stress. This approach will be applied to different materials, from the most famous semiconductor of the twenty-first century, **silicon**, to new promising materials such as **high entropy alloys** that are interesting material, composed by more than five principal elements in equal or near equal atomic percentage[27], and shows promising mechanical properties at the nanoscale.

Appendix A

Supplementary Material

A.1 MD input code

```
#############################################################
                    # NANOPARTICLE
#############################################################



# ---------- Initialize Simulation ---------------------
clear
units metal
dimension 3
boundary p p p
atom_style atomic
atom_modify map array
processors * * *
comm_style tiled

# ---------- Create Atoms ---------------------
read_data Wulff_225977.in
# Ico_309.in Ico_2057.in Ico_5083.in
# Wulff_405.in Wulff_2075.in Wulff_5635.in
# Wulff_26885.in Wulff_83537.in Wulff_225977.in

# ---------- Define Interatomic Potential ---------------------
mass 1 196.96657 #Au
#pair_style eam/alloy
#pair_coeff * * Au.eam.alloy Au
```

```
pair_style smatb
#pair_coeff  id1 id2 atomDiameter p q A Xi cut_start cut_end
pair_coeff 1 1 2.885 10.295370 4.02006 0.205932 1.80239 4.08000612 5.770
neighbor 1 bin
neigh_modify delay 10 check yes
#############################################################
                    # VARIABLES
#############################################################
# ---------- Temperature ----------------------------

variable t equal 0.01 # temperature

timestep 0.001 #pico to femto

#------------ initial position ---------------------
#variable zzero equal 10.20
#variable zzero equal 20.3
#variable zzero equal 28.45
#variable zzero equal 50.9
#variable zzero equal 75.3
variable zzero equal 105.9

#-------------FINAL STRAIN--------------------------
variable strain equal 0.1

#------------- indenter velocity --------------------
variable vel equal -0.0002#step displacement

#------------- Indenter position --------------------
variable zInd equal "v_zzero+v_vel*step*dt"

#------------ Fixed Indenter position ----------------
variable zInd2 equal "- v_zzero+0.1"

#------------   OUTPUT  -------------------------------

variable o equal "v_strain*(round(v_zzero)*2)/(-v_vel*dt)"
#set the final iteration number
variable u1 equal 0.1
#set the printing every [A]
variable u  equal "v_u1/(-v_vel*dt)"
#variable u equal 100

#-------------   Strain Rate  ------------------------
variable sr equal "round(-v_vel/(v_zzero*2*1E-15*1E8))"
#1E-15 unit of time
```

```
#############################################################
                  # ENERGY MINIMIZATION
#############################################################
fix 2 all balance 1000 1.1 rcb #change the processor grid


#fix 1 all box/relax iso 0.0 vmax 0.001
thermo  1000
thermo_style custom step temp spcpu cpuremain
#min_style cg
minimize 1e-25 1e-25 5000 10000
reset_timestep 0
#############################################################
           # NON EQUILIBRIUM INDENTATION
#############################################################

print "Strain rate = ${sr}  1E8;"

#-------------  Surface atoms -----------------------

variable l equal "v_vel*step*dt"
variable b equal "v_zzero - 1" # BOX HEIGHT

region 2 block INF INF INF INF $b INF side in move NULL NULL v_l
group surf dynamic all region 2 every 1
variable N equal count(surf,2)


#############################################################
################       FIX               ###################
#############################################################



# ---------------  COMPUTE  ------------------------
#compute 1 all centro/atom fcc axes yes
#compute 2 all property/atom fz
compute 3 all pe/atom
compute  4 all stress/atom  NULL
compute  5 all voronoi/atom

# ---------------  ENSEMBLE ------------------------

velocity all create $t 12 mom yes rot yes dist gaussian
fix 3 all nvt temp $t $t 1 drag 1
```

```
#fix 3 all npt temp $t $t 1 x 0 0 1 y 0 0 1 drag 2
#fix 3 all nve

# --------------INDENTATION ------------------------
fix 4 all indent 1000 plane z v_zInd hi
fix 6 all indent 1000 plane z v_zInd2 lo


##############################################################
#################       OUTPUT            ###################
##############################################################
thermo  $u
thermo_style custom step temp v_zInd f_4[3] spcpu cpuremain v_N f_6[3]


variable p2 equal "step"
variable p3 equal "v_zInd"
variable p4 equal "f_4[3]"

fix def1 all print $u " ${p2} ${p3} ${p4}" file data.txt screen no

variable a1 equal "c_4[1]/c_5[1]*100000"


dump  1 all cfg $u dump.nvt_*.cfg mass type xs ys zs c_5[1] c_3 c_4[3]
dump_modify 1 element Au

#dump  2 surf cfg $u dump.surf_*.cfg mass type xs ys zs
#dump_modify 2 element Au
dump  3 surf atom $u dump.py_*.txt
dump_modify 3 scale no

#dump  4 all atom $u dump.FE_*.txt
#dump_modify 4 scale no


run $o
#run 1000

#######################################
# SIMULATION DONE
print "All done"
```

A.2 FE input code

```
from __future__ import print_function
from fenics import *
#from dolfin import *
from ufl import nabla_div
import numpy as np
import scipy.spatial
import matplotlib.pyplot as plt
from scipy.spatial import Delaunay
import os

def area_tot(A):
A_tot = 0
for i in range(0,len(A[:,0,0])):
x = A[i,0,0:2]
y = A[i,1,0:2]
z = A[i,2,0:2]
A_tri =((x[0]*(y[1]-z[1])) +(y[0]*(z[1]-x[1])) + (z[0]*(x[1]-y[1])))*0.5
A_tot = A_tot + A_tri

return(A_tot)


mu = 22*1E9
# [Pa] final elastic constant
lambda_ = 167*1E9    # [Pa]
true_strain = 0.05
num_steps = 1



#Define mesh
mesh = Mesh("NP6.xml")
V = VectorFunctionSpace(mesh, 'P', 1)

# Define boundary condition
tol = 1E-14
mesh_coord = mesh.coordinates()
x2_max = np.max(mesh_coord[:,2])
x2_min = np.min(mesh_coord[:,2])
size = x2_max - x2_min
print("Nanoparticle size [nm] : %f"%(size/10))
displ = -size*true_strain #set displacement
```

```
displ_range = np.linspace(displ,displ,num_steps)
stress = [None]*num_steps
strain = [None]*num_steps
E = [None]*num_steps

bmesh = BoundaryMesh(mesh, "exterior")
B = bmesh.coordinates()
R = np.max(B[:,2])
points = np.zeros((len(B[:,2]),3))

# identification of atoms on top surface
j = 0
for i in range(0,len(B[:,2])):
if B[i,2] >= (R-1):
points[j,:] = B[i,:]
j = j +1
C = points[0:j,:]

#function for area calculation
tri = Delaunay(C[:,0:2])
A = points[tri.simplices]
area = area_tot(A)
print("Top facet area: %f"%(area))

#Define top and bottom region
def bot(x,on_boundary):
return on_boundary and (x[2] < (x2_min + 0.25))
def top(x,on_boundary):
return on_boundary and (x[2] > (x2_max - 0.25))


u = TrialFunction(V)
d = u.geometric_dimension()  # space dimension
v = TestFunction(V)



def epsilon(u):
return 0.5*(nabla_grad(u) + nabla_grad(u).T)

def sigma(u):
return lambda_*nabla_div(u)*Identity(d) + 2*mu*epsilon(u)



# extraction of degree of freedom indexes that
```

```
#refer to z in the vectorial space V
# sub(i) Return the i-th sub space 2 --> z
#.dofmap() Access to the degree of freedom
# dofs() Return list of dof indices on
# this process that belong to mesh entities

f =Constant((0, 0, 0))
T =Constant((0, 0, 0))
a = inner(sigma(u), epsilon(v))*dx
L = dot(f, v)*dx + dot(T, v)*ds

for n in range(num_steps):
    Fz = 0
    bc1=DirichletBC(V.sub(2),Constant(0.0),bot)
#displacement at left side
    bc2=DirichletBC(V.sub(2),Constant(displ_range[n]),top)
#displacement at right side
    bc=[bc1,bc2]#,bc3]
#total boundary condition
    u = Function(V)
#linear problem
    solve(a == L, u, bc,solver_parameters={'linear_solver': 'mumps'})
    f_int = assemble(inner(sigma(u), epsilon(v))*dx)
#reaction force calculation only on bc1
    bc1.apply(f_int)
    z_dofs = V.sub(2).dofmap().dofs()
    for i in z_dofs:
        Fz += f_int[i]


stress[n] = Fz/area *1E-9
strain[n] = displ_range[n]/size
E[n] = stress[n]/strain[n]
#print("{:<21}{:<23}".format(strain[n],stress[n])
print("Vertical reaction force: [GN]%f"%(Fz*1E-9))
print("True stress on top facet [GPa] : %f"%(stress[n]))
print("True strain : %f"%(strain[n]))
print("Effective elastic constant [GPa] : %f"%(E[n]))


#print(stress)
#print(strain)
print(E)


# apply displacement to mesh
```

```
ALE.move(mesh, u)


# OUTPUT

V = TensorFunctionSpace(mesh, 'P', 1)
#need a tensor space to project sigma.
s = sigma(u)

stress = project(sigma(u),V,solver_type = "mumps")
strain = project(epsilon(u),V,solver_type = "mumps")
# Save solution to file in VTK format
File('elasticity/displacement_%f.pvd'%(size)) << u
File('elasticity/simga_%f.pvd'%(np.round(size)))   << stress
File('elasticity/epsilon_%f.pvd'%(size))   << strain
```

A.3 Additional figure

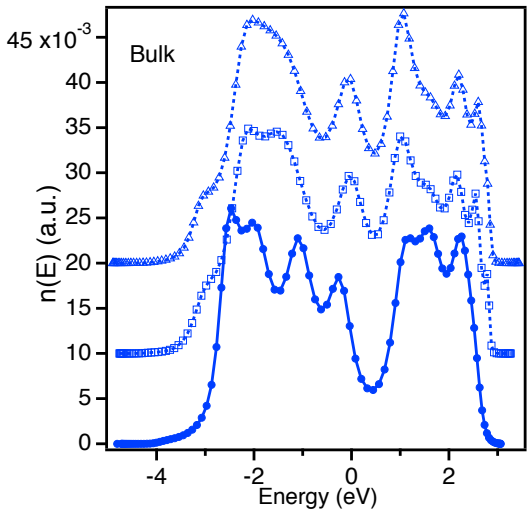

Figure A.1: Under deformation LDOS

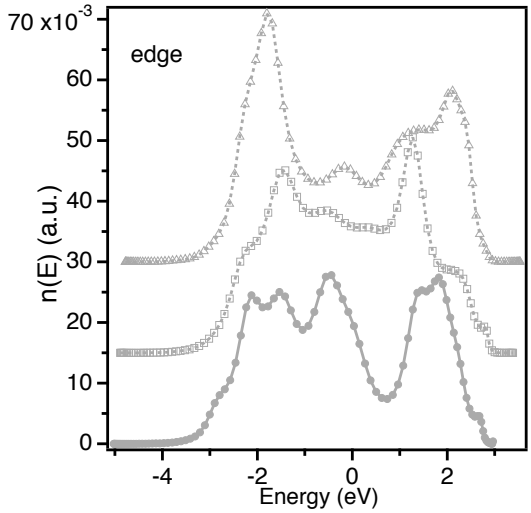

Figure A.2: Under deformation LDOS

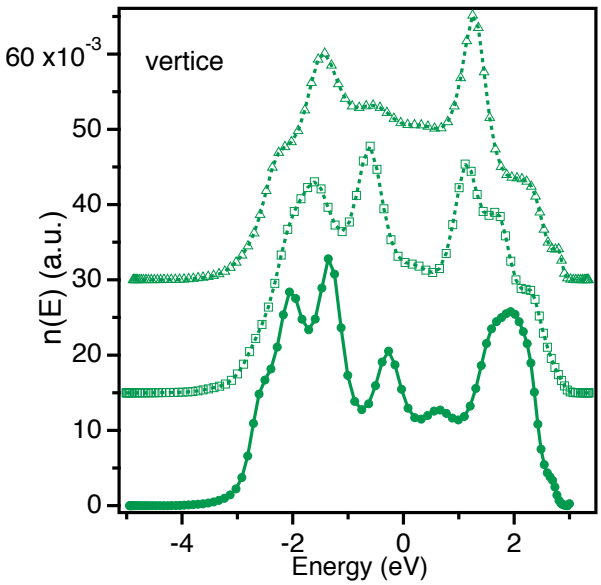

Figure A.3: Under deformation LDOS

Bibliography

[1] Dan Mordehai, Seok Woo Lee, Björn Backes, David J. Srolovitz, William D. Nix, and Eugen Rabkin. «Size effect in compression of single-crystal gold microparticles». In: *Acta Materialia* 59.13 (2011), pp. 5202–5215. ISSN: 13596454. DOI: 10.1016/j.actamat.2011.04.057 (cit. on pp. 1, 14, 16, 19, 20).

[2] S. Roy, R. Gatti, B. Devincre, and D. Mordehai. «A multiscale study of the size-effect in nanoindentation of Au nanoparticles». In: *Computational Materials Science* 162.February (2019), pp. 47–59. ISSN: 09270256. DOI: 10.1016/j.commatsci.2019.02.013 (cit. on pp. 2, 14, 16).

[3] Dan Guo, Guoxin Xie, and Jianbin Luo. «Mechanical properties of nanoparticles: Basics and applications». In: *Journal of Physics D: Applied Physics* 47.1 (2014). ISSN: 00223727. DOI: 10.1088/0022-3727/47/1/013001 (cit. on p. 2).

[4] Daan Frenkel and B Smit. «Understanding Molecular Simulation (Computational Science Series, Vol 1)». In: (2001), p. 664 (cit. on pp. 4, 17).

[5] Steve Plimpton. «Short-Range Molecular Dynamics». In: *Journal of Computational Physics* (1997). DOI: 10.1006/jcph.1995.1039. arXiv: nag.2347. URL: //lammps.sandia.gov/ (cit. on p. 4).

[6] Adrian P. Sutton. *Electronic Structure of Materials - Sutton*. 2004 (cit. on pp. 4, 6).

[7] D.G. Pettifor D.L. Weaire-Springer. DOI: 10.1007/978-3-642-82444-9 (cit. on p. 5).

[8] F. Ducastelle and F. Cyrot-Lackmann. «Moments developments and their application to the electronic charge distribution of d bands». In: *Journal of Physics and Chemistry of Solids* 31.6 (1970), pp. 1295–1306. DOI: https://doi.org/10.1016/0022-3697(70)90134-4 (cit. on pp. 6, 7).

[9] J. Friedel Volker Heine D. Shoenberg. *The Physics of Metals: Volume 1 Electrons*. 2011 (cit. on p. 6).

[10] J.C. Woolley. *Introduction to solid state physics*. Vol. 6. 1. 1957, p. 83. ISBN: 047141526X. DOI: 10.1016/0022-5096(57)90051-0 (cit. on pp. 7–9, 13, 14, 22).

[11] William S Slaughter. *The linearized theory of elasticity*. Vol. 16. C. 1973, pp. 46–78. ISBN: 9781461266082. DOI: 10.1016/S0167-5931(13)70008-1 (cit. on p. 7).

[12] Rob Phillips. *Crystals, Defects and Microstructures: Modeling Across Scales*. Cambridge University Press, 2001. DOI: 10.1017/CBO9780511606236 (cit. on pp. 8, 9).

[13] Martin S. Alnæs et al. «The FEniCS Project Version 1.5». In: *Archive of Numerical Software* 3.100 (2015). DOI: 10.11588/ans.2015.100.20553 (cit. on p. 9).

[14] Anders Logg, Kent-Andre Mardal, Garth N. Wells, et al. *Automated Solution of Differential Equations by the Finite Element Method*. Springer, 2012. ISBN: 978-3-642-23098-1. DOI: 10.1007/978-3-642-23099-8 (cit. on p. 9).

[15] Hans Petter Langtangen and Anders Logg. «Solving PDEs in Minutes - The FEniCS Tutorial Volume I». In: *Manual* I (2016). DOI: 10.1007/978-3-319-52462-7 (cit. on pp. 9, 18).

[16] William T. Thomson and William T. Thomson. «Introduction to the Finite Element Method». In: *Theory of Vibration with Applications* (2018), pp. 301–344. DOI: 10.1201/9780203718841-11 (cit. on p. 10).

[17] *UFL Specification and User Manual 0.3*. Tech. rep. 2010. URL: http://www.fenics.org/ (cit. on p. 10).

[18] Dan Mordehai, Michael Kazakevich, David J. Srolovitz, and Eugen Rabkin. «Nanoindentation size effect in single-crystal nanoparticles and thin films: A comparative experimental and simulation study». In: *Acta Materialia* 59.6 (2011), pp. 2309–2321. ISSN: 13596454. DOI: 10.1016/j.actamat.2010.12.027. URL: http://dx.doi.org/10.1016/j.actamat.2010.12.027 (cit. on pp. 14, 16).

[19] C. E. Carlton and P. J. Ferreira. «In situ TEM nanoindentation of nanoparticles». In: *Micron* 43.11 (2012), pp. 1134–1139. ISSN: 09684328 (cit. on pp. 14, 16).

[20] D. Kilymis, C. Gérard, J. Amodeo, U. V. Waghmare, and L. Pizzagalli. «Uniaxial compression of silicon nanoparticles: An atomistic study on the shape and size effects». In: *Acta Materialia* 158 (2018), pp. 155–166. ISSN: 13596454. DOI: 10.1016/j.actamat.2018.07.063 (cit. on pp. 14, 16, 19, 20).

[21] M. José Yacamán, J. A. Ascencio, H. B. Liu, and J. Gardea-Torresdey. «Structure shape and stability of nanometric sized particles». In: *Journal of Vacuum Science and Technology B: Microelectronics and Nanometer Structures* 19.4 (2001), pp. 1091–1103. ISSN: 10711023. DOI: 10.1116/1.1387089 (cit. on p. 15).

[22] Georgios D Barmparis and Ioannis N Remediakis. *First-principles atomistic Wulff constructions for gold nanoparticles*. Tech. rep. 2012. arXiv: 1111.4667v2. URL: https://wiki.fysik.dtu.dk (cit. on p. 15).

[23] Alexander Stukowski. «Visualization and analysis of atomistic simulation data with OVITO–the Open Visualization Tool». In: *Modelling and Simulation in Materials Science and Engineering* 18.1 (Dec. 2009), p. 015012. DOI: 10.1088/0965-0393/18/1/015012. URL: https://doi.org/10.1088%2F0965-0393%2F18%2F1%2F015012 (cit. on p. 15).

[24] Yosi Feruz and Dan Mordehai. «Towards a universal size-dependent strength of face-centered cubic nanoparticles». In: *Acta Materialia* 103 (2016), pp. 433–441. ISSN: 13596454. DOI: 10.1016/j.actamat.2015.10.027 (cit. on pp. 16, 20).

[25] Tevis D B Jacobs and Ashlie Martini. «Measuring and Understanding Contact Area at the Nanoscale: A Review». In: (2017). DOI: 10.1115/1.4038130 (cit. on p. 17).

[26] Daniel N. Blaschke. «Averaging of elastic constants for polycrystals». In: *Journal of Applied Physics* 122.14 (2017), pp. 1–12. ISSN: 10897550. DOI: 10.1063/1.4993443. arXiv: 1706.07132 (cit. on p. 18).

[27] Yong Zhang, Ting Ting Zuo, Zhi Tang, Michael C. Gao, Karin A. Dahmen, Peter K. Liaw, and Zhao Ping Lu. «Microstructures and properties of high-entropy alloys». In: *Progress in Materials Science* 61.November 2013 (2014), pp. 1–93. ISSN: 00796425. DOI: 10.1016/j.pmatsci.2013.10.001. URL: http://dx.doi.org/10.1016/j.pmatsci.2013.10.001 (cit. on p. 25).